Anion Reduction Dominated Cathodic Limit of Metal–Free Ionic Liquid: Experimental and Theoretical Proofs

ARTICLE *in* THE JOURNAL OF PHYSICAL CHEMISTRY B · OCTOBER 2013

Impact Factor: 3.3 · DOI: 10.1021/jp408631p · Source: PubMed

6 AUTHORS, INCLUDING:

Hsing-Yin Chen
Kaohsiung Medical University
43 PUBLICATIONS **835** CITATIONS
SEE PROFILE

Chi-Yu Lu
Kaohsiung Medical University
62 PUBLICATIONS **408** CITATIONS
SEE PROFILE

Po-Yu Chen
Kaohsiung Medical University
60 PUBLICATIONS **1,585** CITATIONS
SEE PROFILE

THE JOURNAL OF PHYSICAL CHEMISTRY B

Article

pubs.acs.org/JPCB

Anion Reduction Dominated Cathodic Limit of Metal-Free Ionic Liquid: Experimental and Theoretical Proofs

Nai-Chang Lo,[†] Hsing-Yin Chen,*[,†] Wan-Jung Chuang,[†] Chi-Yu Lu,[‡] Ping-Yu Chen,[§] and Po-Yu Chen*[,†]

[†]Department of Medicinal and Applied Chemistry, Kaohsiung Medical University, Kaohsiung 807, Taiwan

[‡]Department of Biochemistry, Kaohsiung Medical University, Kaohsiung 807, Taiwan

[§]Department of Chemistry, National Chung Hsing University, Taichung 402, Taiwan

Supporting Information

ABSTRACT: The cathodic limit of the electrochemical window in the second-generation ionic liquids (composed of air- and water-stable metal-free cations and anions) is traditionally believed to be determined by the reduction of the cation. More and more exceptions, however, were found in various ionic liquids. In this study, the cathodic limit of the electrochemical window in 1-butyl-1-methylpyrrolidinium salicylate ionic liquid (BMP-SAL IL) was studied. It has been found that the cathodic limit of BMP-SAL is determined by the reduction of SAL^- anion rather than the reduction of BMP^+ cation. The cyclic voltammetric behavior, NMR spectra, and MALDI-TOF MS spectra of BMP-SAL recorded before and after the IL was electrolyzed at the cathodic limit provide sufficient evidence that the major reaction at the cathodic limit of BMP-SAL is the reduction of SAL^- anion. The theoretical calculations support the experimental data, and the results indicate that anion reduction dominated cathodic limit should be a common phenomenon in ionic liquids.

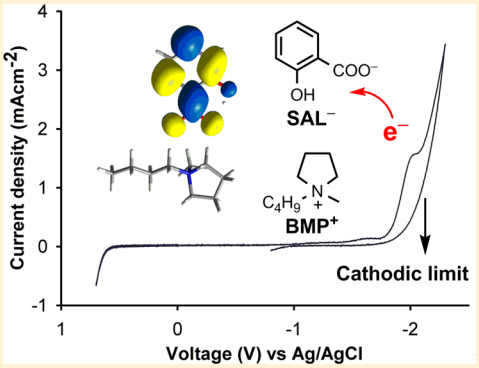

1. INTRODUCTION

Ionic liquids, especially room temperature ionic liquids (RTILs), have been widely studied and used for many applications. Because of their inherent ionic conductivity, ILs have been extensively used for electrochemical studies.[1,2] For electrochemical applications, the electrochemical stability of the ILs (i.e., the width of the electrochemical window) is always an important factor that determines whether an electrochemical reaction is able to be studied in a particular ionic liquid. It, therefore, is important to know where the cathodic and anodic limits locate and what reactions occur at the limits. Recently, the second-generation ILs, which are composed of air- and water-stable cations such as imidazolium, pyrrolidinium, ammonium, and phosphonium and anions such as BF_4^-, PF_6^-, and imide type anions, are mostly used. It is believed conventionally that the cathodic limits of the electrochemical windows in these ILs are determined by the reduction of the cations[3−5] and the oxidation of the anions determines the anodic limits.[3,6,7] However, recent experiments have indicated that this may not always be true. It has been demonstrated by the experimental and theoretical investigations that bis-((trifluoromethyl)sulfonyl)imide (TFSI) anion, which has been commonly used for the preparation of ILs, undergoes reductive decomposition.[8] This unusual behavior recently has been further approved by *in situ* electrochemical X-ray photoelectron spectroscopy[9] and in situ FTIR study.[10] Actually, the reduction of anionic species at the cathodic limit is not quite uncommon for the metal halide-based first-generation ILs. For instance, the cathodic limit results from the reduction of the heptachloroaluminate ($Al_2Cl_7^-$) anion in the Lewis acidic chloroaluminate-based ILs.[3−5,11] However, the strong Lewis acidic $Al_2Cl_7^-$ anion is deficient of electrons, which is traditionally believed to accept electrons more easily than the Lewis basic TFSI anion; the reduction of the latter at the cathodic limit is thus considered unusual. It has been reported that molecular dynamics and density functional theory (DFT) calculations might be good tools to predict the species involved in the limits of the electrochemical windows.[12] By taking all interior interactions into account, the calculated energies of the highest occupied molecular orbital (HOMO) and the lowest unoccupied molecular orbital (LUMO) can provide a criterion for predicting the likely species contributing to reductive (cathodic limit) and oxidative (anodic limit) decomposition.

Although the atypical anion reduction has been mentioned in the literature and theoretical calculations support the observations, there is still a lack of direct experimental observation of anion reduction. In this study, the cathodic limit of the new room temperature ionic liquid 1-butyl-1-methylpyrrolidinium salicylate (BMP-SAL) was studied by cyclic voltammetry, nuclear magnetic resonance spectroscopy (NMR), and matrix-assisted laser desorption-ionization time-of-flight mass spectrometry (MALDI-TOF MS) before and after carrying out the potentiostatic electrolysis by applying a reduction potential at the cathodic limit. The aromatic SAL^-

Received: August 28, 2013
Revised: October 9, 2013
Published: October 9, 2013

anion was seldom used for forming ILs,[13−15] but 1-butyl-3-methylimidazolium salicylate (BMI-SAL) has been previously used for the electrodeposition of copper.[16] BMP-SAL is a new IL, and it is interesting to understand its fundamental properties. The aromatic SAL^- anion seems to be easily reduced to a stable anionic radical in accordance with the experimental results. The cathodic limit of BMP-SAL, therefore, was determined by the reduction of SAL^- anion. Theoretical calculations were also performed, and the results support the experimental data. This study approves the previous report[12] and provides experimental evidence to change our traditional concepts about the species of ILs involving in the potential limits of the electrochemical windows.

2. EXPERIMENTAL SECTION

2.1. Materials and Apparatus. 1-Butyl-1-methylpyrrolidinium salicylate ionic liquid (BMP-SAL IL) was prepared by following our previously reported procedures.[16] However, 1-butyl-1-methylpyrrolidinium chloride (BMPCl) was used, which was prepared by following the published method[17] but chlorobutane (Aldrich, 99.5%) was used in this study. Briefly, the BMP-SAL was prepared by mixing BMPCl and sodium salicylate (NaSAL, Alfa Aesar, 99%) in equal moles in dried acetonitrile. NaCl precipitates produced during the metathesis were filtered off to leave the BMP-SAL/acetonitrile solution. After removing the acetonitrile by vacuum, the as-prepared BMP-SAL was dried under a vacuum at 120 °C for at least 1 day using a diffusion pump and then stored in a nitrogen-filled glovebox.

Cyclic voltammetry and potentiostatic electrolysis were performed with a potentiostat/galvanostat (Princeton Applied Research, PAR 263A) under a purified nitrogen atmosphere in a glovebox (MBraun, UNI-LAB B) in which the moisture and oxygen were maintained below 1 ppm. A conventional one-compartment three-electrode cell was used for all electrochemical experiments, and the solution temperature was controlled at 70 °C. The reference electrode was Ag/AgCl in 1-butyl-1-methylpyrrolidinium bis((trifluoromethyl)sulfonyl)-imide ionic liquid (BMP-TFSI IL) dissolved with 1 M BMPCl in a glass tube with a porous Vycor tip. A platinum spiral immersed in BMP-TFSI IL[17] and separated from the bulk solution by a porosity E glass frit was used as the counter electrode. For cyclic voltammetric experiments, a platinum disk electrode (1.6 mm ø) was used as the working electrode. The working electrode was a piece of platinum foil (1.9 × 2.4 cm^2) for the potentiostatic electrolysis. A nuclear magnetic resonance spectrometer (NMR, Varian, UNITY Plus 400) and matrix assisted laser desorption-ionization time-of-flight mass spectrometer (MALDI-TOF MS equipped with a 355 nm Nd:YAG laser, Bruker Daltonics, Autoflex III Smartbeam) were used to study BMP-SAL IL before and after the IL was potentiostatically electrolyzed at the cathodic limit.

2.2. Potentiostatic Electrolysis of BMP-SAL at the Cathodic Limit. In order to study the cathodic limit of the electrochemical window in BMP-SAL, potentiostatic electrolysis was carried out by applying a potential of −2.3 V where the cathodic limit of BMP-SAL was observed. After passing a particular quantity of charges, the electrolyzed BMP-SAL was diluted with deuterated dimethylsulfoxide (d_6-DMSO, Aldrich, 99.9%) for NMR measurements. However, the electrolyzed IL (1 μL) was directly used for MALDI-TOF MS experiments without a matrix. The 1 μL of IL was added on a stainless steel plate, and then, MS spectra were acquired in positive or negative ion reflector mode for the summing of 1000 laser shots. Data was processed by FlexAnalysis software.

2.3. Theoretical Calculations. The B3LYP and M06-2X functionals in combination with 6-31+G* and 6-31++G** basis sets were employed in the present density functional theory (DFT) calculations. The B3LYP functional has been shown to be adequate for evaluating molecular electron affinities (EAs)[18] and, therefore, was selected in this study to investigate the variation of EAs of BMP^+ and SAL^- with the dielectric constant of the surrounding medium. On the other hand, the M06-2X functional is superior to the B3LYP in describing intermolecular interactions.[19] Accordingly, we used the M06-2X functional to explore the properties of the BMP^+-SAL^- complex. Frequency calculations were carried out at the same level of theory as geometry optimizations for the examination of the nature of the optimized structures and for thermal corrections to Gibbs free energies (298 K and 1 atm). The effect of the surrounding medium was taken into account by using the SMD continuum solvation model.[20] Geometry optimizations and frequency calculations were performed under the SMD solvation model. The adiabatic electron affinity and ionization potential (IP) were evaluated by the definition EA = $E_n - E_{n+1}$ and IP = $E_{n-1} - E_n$, respectively, where n denotes the number of molecular electrons. All the calculations were carried out with Gaussian 09 program.[21]

3. RESULTS AND DISCUSSION

3.1. Cyclic Voltammetric Behavior of BMP-SAL. The IL used in this study is a light yellow viscous liquid. Although we did not measure its viscosity, it shows a more viscous behavior over the BMP-TFSI and BMP-DCA (DCA: dicyanamide) ILs.[22,23] The cyclic voltammogram (CV) of BMP-SAL recorded at a platinum disk electrode was shown in Figure 1A. This CV

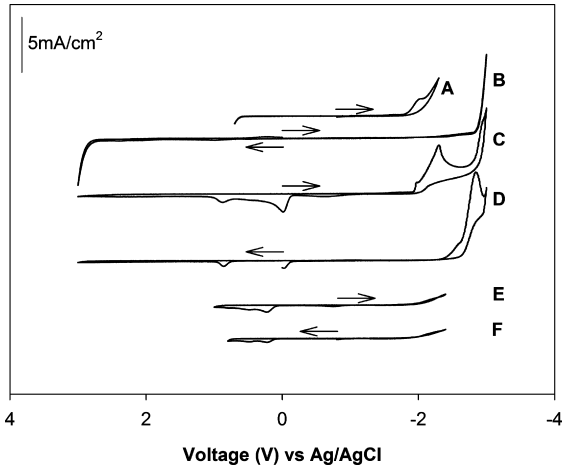

Figure 1. Cyclic voltammograms recorded at the Pt electrode in (A) neat BMP-SAL, (B) neat BMP-TFSI, (C, D) BMP-TFSI containing 0.55 mol % BMP-SAL, and (E, F) BMP-SAL being electrolyzed at −2.3 V for passing 43.24 C of charge. Arrows indicate the initial scan direction. Scan rate: 0.05 V s^{-1}. Temperature: 343 K.

is actually a combination of two CVs where the potential was scanned from the initial potential (−0.8 V) in the cathodic or the anodic direction, respectively, in order to prevent the multiple redox waves that result from the redox reactions of the species produced at the cathodic or anodic limits. It can be found that the electrochemical window of BMP-SAL is very

dx.doi.org/10.1021/jp408631p | J. Phys. Chem. B 2013, 117, 13899−13905

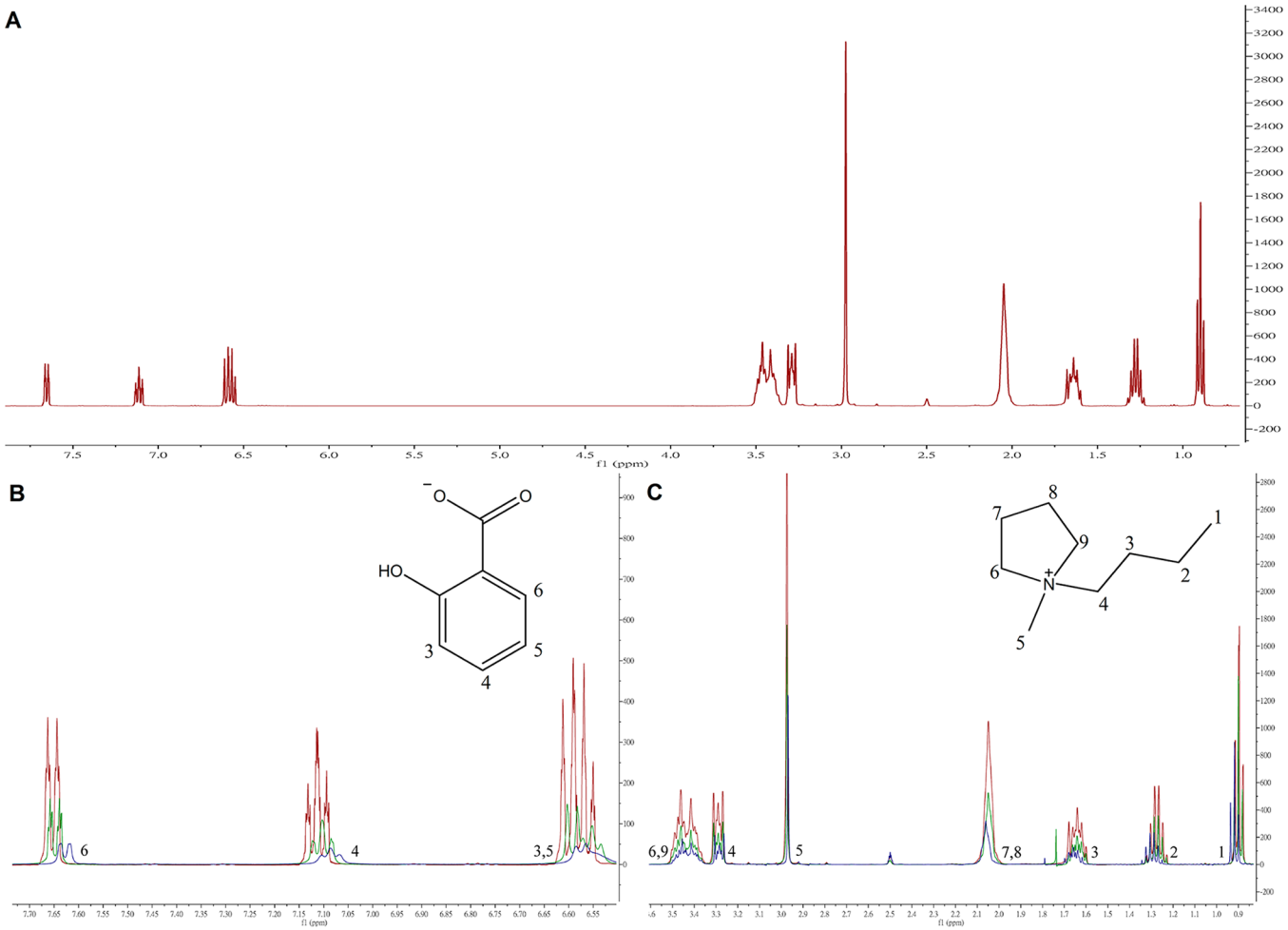

Figure 2. NMR spectra of (A) neat BMP-SAL, (B) SAL^- anion, and (C) BMP^+ cation. Green and blue curves respectively demonstrate the NMR spectra of BMP-SAL being electrolyzed at −2.3 V for passing 25 and 41 C of charge. Solvent: d_6-DMSO.

narrow (about 2.54 V; +0.60 to −1.94 V), compared with those of other BMP-based ILs such as BMP-TFSI. Traditionally, the anodic limit is believed to be resulting from the oxidation of the anion. It is thus supposed that the anodic limit of BMP-SAL results from the oxidation of SAL^-. The working electrode was passivated after the potential was scanned over the anodic limit. This behavior will be shortly discussed in the following. However, this study focuses on the cathodic limit of BMP-SAL. Further investigation on the anodic limit is omitted. In order to prove that the cathodic limit of BMP-SAL results from the reduction of SAL^- rather than BMP^+, cyclic voltammetry was performed in BMP-TFSI with or without the introduction of BMP-SAL. The CV of BMP-TFSI recorded on a Pt electrode is shown in Figure 1B. The potential was scanned from the initial potential of 0.0 V in the cathodic direction, and the switching potentials were −3.0 and +3.0 V, respectively. The extremely wide electrochemical window (over 5 V) and the much more negative cathodic limit imply that the cathodic limit of BMP-SAL is not caused by the reduction of BMP^+ because both ILs are composed of BMP^+ cation. 0.55 mol % of BMP-SAL was introduced into the neat BMP-TFSI, and then, two CVs as shown in Figure 1C,D were recorded. Figure 1C was initially scanned in the cathodic direction, and a reductive wave with peak potential $E_{p,c}$ of −2.3 V was observed. The reductive wave occurred at the potential close to the cathodic limit of BMP-SAL and should result from the reduction of the introduced SAL^- anion. In the reversed scan, two anodic waves ($E_{p,a}$ = −0.012 and +0.872 V) were observed. The first one results from the oxidation of the species that was produced at the cathodic limit, and the second one is due to the oxidation of the introduced SAL^- ion because the second anodic wave is very close to the anodic limit of BMP-SAL IL. No anodic limit can be observed because the working electrode was passivated by the oxidation of SAL^- anion. The same behavior is also observed in Figure 1D where the potential was initially scanned in the anodic direction. The small anodic wave represents the oxidation of SAL^- anion. In the reversed scan, the passivating layer on the electrode surface might be reduced or the layer hindered the reduction of SAL^- anion because the reductive wave was observed at a more negative potential ($E_{p,c}$ = −2.844 V), compared with Figure 1C. However, the cathodic limit of BMP-TFSI did not change. It is emphasized here that a glassy carbon (GC) electrode demonstrated a similar behavior except higher overpotentials were needed for the relevant redox reactions because a slower charge transfer rate is always observed at the GC electrode. Therefore, the reduction of SAL^- anion at the cathodic limit is not only observed at the Pt electrode.

In summary, the CVs shown in Figure 1 indicate that the cathodic limit of BMP-SAL should be determined by the reduction of SAL^- anion instead of the reduction of BMP^+ cation. The latter was traditionally believed determining the

dx.doi.org/10.1021/jp408631p | J. Phys. Chem. B 2013, 117, 13899−13905

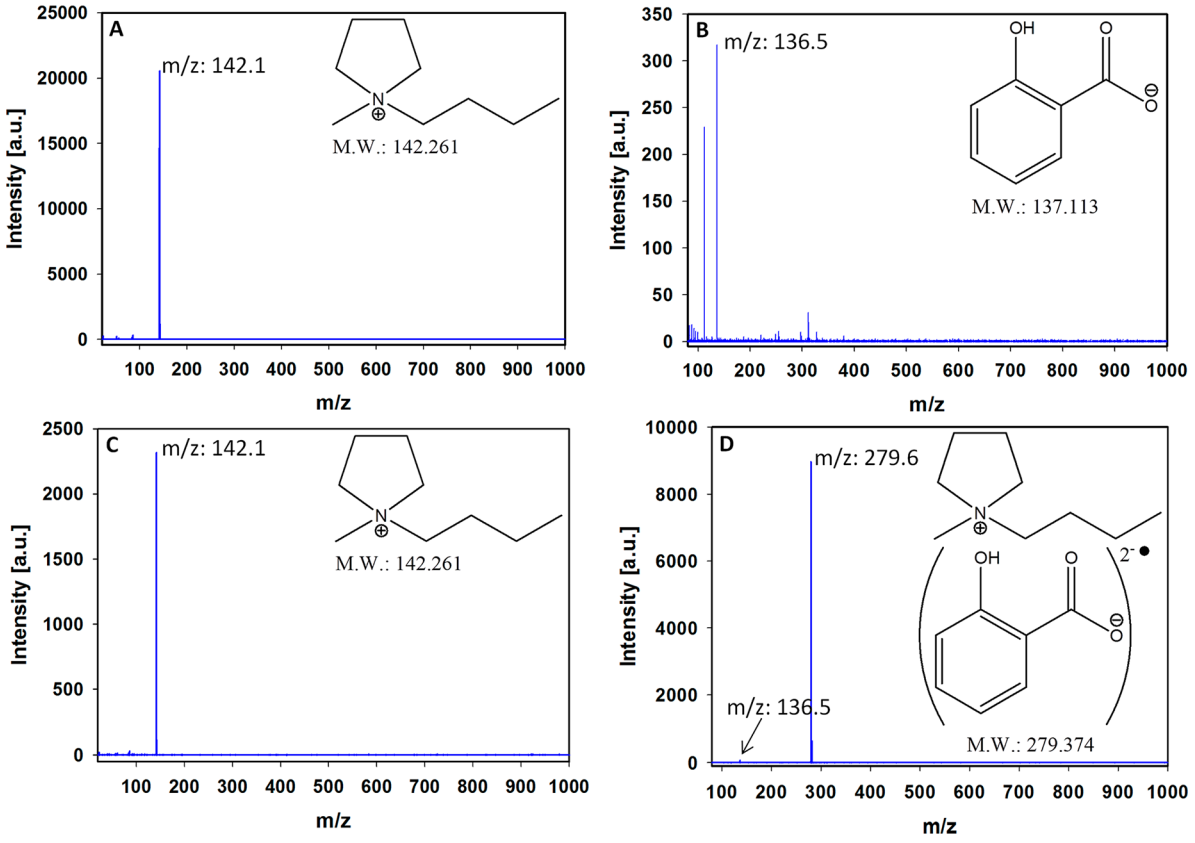

Figure 3. MALDI-TOF MS of BMP-SAL (A, B) before and (C, D) after being electrolyzed at −2.3 V for passing 41 C of charge. (A, C) positive ion mode and (B, D) negative ion mode.

cathodic limit of BMP^+-based ILs. The potentiostatic electrolysis was carried out at −2.3 V where the cathodic limit of BMP-SAL was observed in order to obtain more solid evidence to confirm the reduction of SAL^- anion. After passing a charge of 43.41 C (by assuming one-electron reduction of SAL^- anion, this charge corresponds to a conversion of 3.9% SAL^-), two CVs as shown in Figure 1E,F were recorded. In spite of the initial direction of the potential scan, the onset potential of the cathodic limit slightly shifted to the more negative potential and two new anodic waves were observed. After the electrolysis, the voltammetric behavior of BMP-SAL obviously changed but no further information can be provided. Therefore, NMR and MS spectrometry were performed and the relevant results are provided in the following.

3.2. NMR Spectrometric Investigations. NMR spectra were obtained before and after the BMP-SAL IL was electrolyzed at −2.3 V by passing a charge of 25 and 41 C, respectively. The relevant spectra are demonstrated in Figure 2. Figure 2A represents the complete spectrum of neat BMP-SAL. The signals with chemical shifts (δ) higher than 6.5 correspond to the aromatic hydrogen atoms (i.e., the H atoms at the SAL^- anion). The signals with δ lower than 3.5 represent the H atoms at the BMP^+ cation. Hydrogen atoms at different carbon sites are assigned with the relevant numbers, which are shown in the figure. The ratios of the integrated peak areas represent the numeric ratios of the hydrogen atoms. The results indicate that the numbers of hydrogen atoms are correct in accordance with the chemical structure of BMP-SAL.

The green curve shown in Figure 2 is the NMR spectrum obtained after the IL was electrolyzed by passing a charge of 25 C. It is apparent that the H signals of the SAL^- anion shift toward the high-field direction accompanied by peak broadening. By passing more charges up to 41 C, the signals more extensively shift to the high-field direction and the peak broadening is more obvious (see the blue curve in Figure 2). On the other hand, the NMR spectra of the BMP^+ cation did not show such an obvious dependence on electrolysis; the changes are still observable. After the IL was electrolyzed, the chemical shifts of the H atoms located around the N^+ atom (i.e., H atoms at number 4, 5, 6, and 9 carbons of BMP^+) very slightly shifted to the high-field direction with no peak broadening (the blue curve in Figure 2). The shifting direction, however, is different (toward the low-field) for the H atoms connected to the carbons far away the N^+ atom (i.e., H atoms at number 1, 2, 3, 7, and 8 carbons; blue curve in Figure 2).

The above behavior implies that electrons were delivered from the working electrode to the SAL^- anions when BMP-SAL was electrolyzed at the cathodic limit. If one electron is transferred to one SAL^- anion, the electron density of the aromatic ring must increase, leading to the high-field shift of the aromatic H atoms (number 3, 4, 5, and 6 hydrogens of SAL^-). In addition, the peaks of aromatic H atoms significantly broadened after the electrolysis, which is evidence of radical formation.[24] A radical should be formed ($SAL^{2-\bullet}$) after one electron is transferred to the SAL^- anion. The electron paramagnetic resonance (EPR) spectrum of BMP-SAL IL in the Supporting Information also provides the verification of radical formation after the IL was electrolyzed at the cathodic limit. On the other hand, the BMP^+ cation shows insignificant shifts of H atom signals and no peak broadening, indicating that BMP^+ cations did not receive electrons during the cathodic electrolysis. The tiny shifts of H signals at the BMP^+ cation may

dx.doi.org/10.1021/jp408631p | J. Phys. Chem. B 2013, 117, 13899−13905

result from the interactions between the BMP^+ cation and the anionic radical $SAL^{2-\bullet}$. It is expectable that the interaction between BMP^+ and $SAL^{2-\bullet}$ is stronger than that between BMP^+ and SAL^-. However, it is not easy to explain why the H atoms of the BMP^+ ion had a different shifting direction after the IL was electrolyzed. Theoretical calculations are able to explain this behavior, and the detail will be provided in the following.

3.3. MALDI-TOF MS Investigations. The BMP-SAL IL can be successfully ionized with or without the matrix, and the obtained spectra are almost identical. The MS spectra shown in the following were obtained without a matrix. The MS spectra obtained in positive ion and in negative ion modes, respectively, for the neat BMP-SAL IL were shown in Figure 3A,B. In positive mode (Figure 3A), the major signal is observed at m/z = 142.1, which is very close to the m/z of singly charged BMP^+ cation (MW = 142.261). In negative mode (Figure 3B), the peak at m/z = 136.5 should be related to the singly charged SAL^- anion (MW = 137.113). After electrolysis, the signal observed in positive mode has no change (Figure 3C, m/z = 142.1), indicating that BMP^+ ion was not reduced during the cathodic electrolysis. However, in negative mode (Figure 3D), it is surprising that a negatively charged species with m/z = 279.6 was observed. This species corresponds to the singly charged ion pair of $[BMP^+\text{-}SAL^{2-\bullet}]^-$ (MW = 279.375). This species may be a solid proof supporting that the reduction of SAL^- anion determines the cathodic limit of BMP-SAL. This result also supports the NMR spectra; the interaction between BMP^+ and $SAL^{2-\bullet}$ should be stronger than that between BMP^+ and SAL^-. Therefore, the ion pair $[BMP^+\text{-}SAL^{2-\bullet}]^-$ can be observed in the MALDI-TOF MS spectra. The signal with m/z = 136.5, which corresponds to the singly charged SAL^- anion, is still observable in Figure 3D.

3.4. DFT Calculations. The calculated IP and EA of isolated BMP^+ and SAL^- embedded in the medium with different dielectric constants are presented in Figures 4 and 5. It can be seen that the IP of BMP^+ dramatically decreases from 14.1 eV at the dielectric constant ε = 0 (i.e., gas phase) to 9.2 eV at ε = 5 and then moderately decreases to a steady value of 8.3 eV at ε = 20, whereas the IP of SAL^- moderately increases from 4.1 eV at ε = 0 to a steady value of 5.3 eV at ε = 20

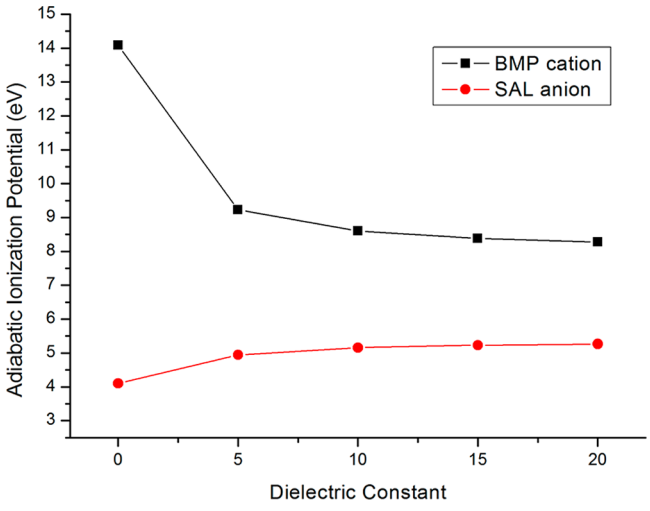

Figure 4. Variation of adiabatic ionization potential with the dielectric constant of the surrounding medium calculated at the B3LYP/6-31+ +G** level.

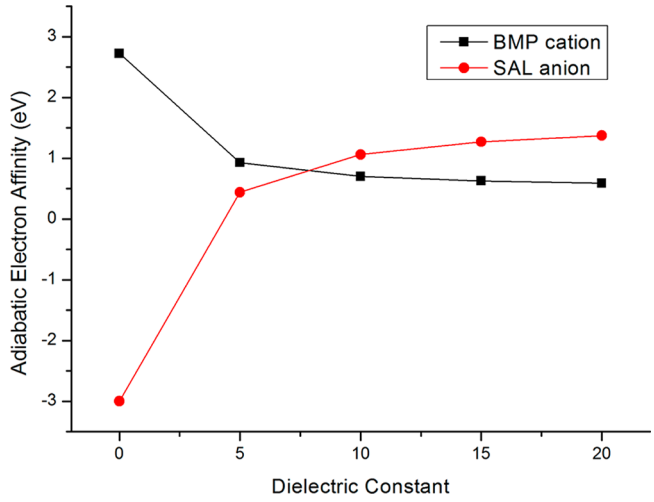

Figure 5. Variation of adiabatic electron affinity with the dielectric constant of the surrounding medium calculated at the B3LYP/6-31+ +G** level.

(Figure 4). Since the IP of BMP^+ is considerably larger than that of SAL^- within the whole range of ε investigated, it is safe to conclude that the anodic limit of BMP-SAL IL is determined by the oxidation of SAL^- anion. In contrast, as the ε of the surrounding medium increases, the EA of BMP^+ and SAL^- respectively decreases from 2.7 to 0.6 eV and increases from −3.0 to 1.4 eV with the magnitude of EA being reversed within the range of ε = 5−10 (Figure 5). It has been reported that the dielectric constants of room-temperature ionic liquids fall in the range 8.8−15.2.[25,26] Accordingly, the EA calculations appear to suggest that the reduction of the BMP-SAL IL takes place on the SAL^- anion rather than on the BMP^+ cation. According to Koopmans' theorem, the IP and EA of a molecule can be approximated by the negative of the highest occupied molecular orbital (HOMO) and lowest unoccupied molecular orbital (LUMO) energies, respectively. Additional analyses of the variations of the negative HOMO and LUMO energies against the dielectric constant were carried out (Supporting Information). Although the absolute values are somewhat different, the variational trends are in agreement with the more accurate IP and EA calculations, supporting that the reduction occurs at the SAL anion when ε > 5.

To verify the above inference, we further studied the reductive behavior of the model complex of $BMP^+\text{-}SAL^-$. Two conformations of the $BMP^+\text{-}SAL^-$ complex and its one-electron adduct $[BMP^+\text{-}SAL^{2-\bullet}]^-$ were located (Figure 6). While conformation **A** is characterized by a perpendicular structure in which the SAL^- uses only the oxygen atoms of the carbonyl group to interact with the BMP^+, conformation **B** adopts a parallel arrangement in which an extended contact between the aromatic ring of SAL^- and the alkyl chain of BMP^+ exists. An inspection of the singly occupied molecular orbital (SOMO) of $[BMP^+\text{-}SAL^{2-\bullet}]^-$ clearly reveals that at the gas phase (ε = 0) the excess electron occupies the diffuse Rydberg orbital of the BMP^+. However, when the influence of the surrounding medium (ε = 5) was taken into account, the excess electron instead entered the π^* orbital of SAL^-. These results are consistent with the prediction from the EA calculations that the magnitude of the EA of BMP^+ and SAL^- starts to reverse at ε > 5.

dx.doi.org/10.1021/jp408631p | J. Phys. Chem. B 2013, 117, 13899−13905

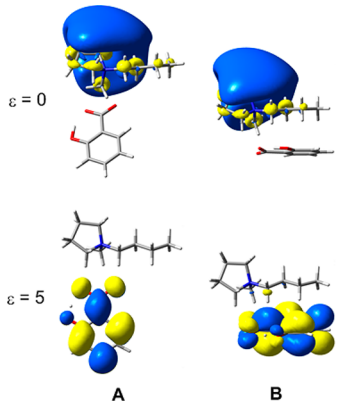

Figure 6. SOMO of $[BMP^+\text{-}SAL^{2-\bullet}]^-$ calculated at the M06-2X/6-31+G* level.

We also calculated the binding free energy ΔG_{bind} of BMP^+-SAL^- and $[BMP^+\text{-}SAL^{2-\bullet}]^-$ immersed in the medium of $\varepsilon = 5$. The former and the latter were evaluated according to the definition $G(BMP^+\text{-}SAL^-) - G(BMP^+) - G(SAL^-)$ and $G([BMP^+\text{-}SAL^{2-\bullet}]^-) - G(BMP^+) - G(SAL^{2-\bullet})$, respectively. The ΔG_{bind} value of $[BMP^+\text{-}SAL^{2-\bullet}]^-$ was found to be considerably larger than that of BMP^+-SAL^- (−16.8 vs −7.0 kcal/mol for conformation **A** and −19.4 vs −6.4 kcal/mol for conformation **B**), obviously due to the stronger electrostatic attraction between monocation BMP^+ and dianion $SAL^{2-\bullet}$. The substantially enhanced ΔG_{bind} of $[BMP^+\text{-}SAL^{2-\bullet}]^-$ rationalizes its appearance in the negative mode of the MS spectrum after electrolysis of the BMP-SAL IL.

4. CONCLUSIONS

Ionic liquids have been utilized in many fields. Their basic properties, however, still need to be discovered. The traditional concepts have been approved that they are not always true in ionic liquids. This study further demonstrates that "unusual behavior" is actually normal in ionic liquids even in environments with higher dielectric constants because the cathodic limit of the electrochemical window in an ionic liquid may be determined by the reduction of anion rather than the reduction of cation; the latter is traditionally believed to be the reaction occurring at the cathodic limit. This study shows that experiments can reveal what species cation or anion determines the limits of electrochemical windows and theoretical calculations are good tools to explain why the experimental results are observed. For studying or utilizing ionic liquids, we need to keep in mind that traditional concepts may be incorrect in ionic liquids.

■ ASSOCIATED CONTENT

Ⓢ Supporting Information

EPR spectrum of the ionic liquid that has been electrochemically reduced and variation of HOMO and LUMO energy with dielectric constant. This material is available free of charge via the Internet at http://pubs.acs.org.

■ AUTHOR INFORMATION

Corresponding Authors

*E-mail: hychen@kmu.edu.tw. Phone: +886-7-3121101, ext. 2587. Fax: +886-7-3125339.

*E-mail: pyc@kmu.edu.tw. Phone: +886-7-3121101, ext. 2587. Fax: +886-7-3125339.

Notes

The authors declare no competing financial interest.

■ ACKNOWLEDGMENTS

The authors thank the the National Science Council of Taiwan (Grant No. NSC 101-2113-M-037-001-MY3) for financial support and the National Center for High-Performance Computing for computer time and facilities. The Center for Resources, Research and Development (Kaohsiung Medical University) is also acknowledged for instrumental support.

■ REFERENCES

(1) Ohno, H. *Electrochemical Aspects of Ionic Liquids*; John Wiley & Sons: Hoboken, NJ, 2005.

(2) Endres, F.; Abbott, A. P.; MacFarlane, D. R. *Electrodeposition From Ionic Liquids*; Wiley-VCH: Weinheim, Germany, 2008.

(3) Bonhote, P.; Dias, A.-P.; Papageorgiou, N.; Kalyanasundaram, K. Hydrophobic, Highly Conductive Ambient-Temperature Molten Salts. *Inorg. Chem.* **1996**, *35*, 1168−1178.

(4) Fuller, J.; Carlin, R. T.; Osteryoung, R. A. The Room Temperature Ionic Liquid 1-Ethyl-3-methylimidazolium Tetrafluoroborate: Electrochemical Couples and Physical Properties. *J. Electrochem. Soc.* **1997**, *144*, 3881−3886.

(5) Nanjundiah, C.; McDevitt, S. F.; Koch, V. R. Differential Capacitance Measurements in Solvent-Free Ionic Liquids at Hg and C Interfaces. *J. Electrochem. Soc.* **1997**, *144*, 3392−3397.

(6) Suarez, P. A. Z.; Selbach, V. M.; Dullius, J. E. L.; Einloft, S.; Piatnicki, C. M. S.; Azambuja, D. S.; de Souza, R. F.; Dupont, J. Enlarged Electrochemical Window in Dialkyl-imidazolium Cation Based Room-Temperature Air and Water-stable Molten Salts. *Electrochim. Acta* **1997**, *42*, 2533−2535.

(7) Koch, V. R.; Dominey, L. A.; Nanjundiah, C.; Ondrechen, M. J. The Intrinsic Anodic Stability of Several Anions Comprising Solvent-Free Ionic Liquids. *J. Electrochem. Soc.* **1996**, *143*, 798−803.

(8) Howlett, P. C.; Izgorodina, E. I.; Forsyth, M.; MacFarlane, D. R. Electrochemistry at Negative Potentials in Bis-(trifluoromethanesulfonyl)amide Ionic Liquids. *Z. Phys. Chem.* **2006**, *220*, 1483−1493.

(9) Wibowo, R.; Aldous, L.; Jacobs, R. M. J.; Manan, N. S. A.; Compton, R. G. In situ Electrochemical-X-ray Photoelectron Spectroscopy: Rubidium Metal Deposition from An Ionic Liquid in Competition with Solvent Breakdown. *Chem. Phys. Lett.* **2011**, *517*, 103−107.

(10) Markevich, E.; Sharabi, R.; Borgel, V.; Gottlieb, H.; Salitra, G.; Aurbach, D.; Semrau, G.; Schmidt, M. A. In situ FTIR Study of the Decomposition of N-butyl-N-methylpyrrolidinium Bis-(trifluoromethanesulfonyl)amide Ionic Liquid during Cathodic Polarization of Lithium and Graphite Electrodes. *Electrochim. Acta* **2010**, *55*, 2687−2696.

(11) Wasserscheid, P.; Welton, T. *Ionic Liquids in Synthesis*; Wiley-VCH Verlag: Weinheim, Germany, 2003.

(12) Ong, S. P.; Andreussi, O.; Wu, Y.; Marzari, N.; Ceder, G. Electrochemical Windows of Room-Temperature Ionic Liquids from Molecular Dynamics and Density Functional Theory Calculations. *Chem. Mater.* **2011**, *23*, 2979−2986.

(13) Egorov, V. M.; Smirnova, S. V.; Pletnev, I. V. Highly Efficient Extraction of Phenols and Aromatic Amines into Novel Ionic Liquids Incorporating Quaternary Ammonium Cation. *Sep. Purif. Technol.* **2008**, *63*, 710−715.

(14) Vendilo, A. G.; Djigailo, D. I.; Smirnova, S. V.; Torocheshnikova, I. I.; Popov, K. I.; Krasovsky, V. G.; Pletnev, I. V. 18-Crown-6 and Dibenzo-18-crown-6 Assisted Extraction of Cesium from Water into Room Temperature Ionic Liquids and Its Correlation with Stability Constants for Cesium Complexes. *Molecules* **2009**, *14*, 5001−5016.

(15) Egorov, V. M.; Djigailo, D. I.; Momotenko, D. S.; Chernyshov, D. V.; Torocheshnikova, I. I.; Smirnova, S. V.; Pletnev, I. V. Task-

specific Ionic Liquid Trioctylmethylammonium Salicylate as Extraction Solvent for Transition Metal Ions. *Talanta* **2010**, *80*, 1177−1182.
(16) Chen, P.-Y.; Chang, Y.-T. Voltammetric Study and Electrodeposition of Copper in 1-Butyl-3-methylimidazolium Salicylate Ionic Liquid. *Electrochim. Acta* **2012**, *75*, 339−346.
(17) MacFarlane, D. R.; Meakin, P.; Sun, J.; Amini, N.; Forsyth, M. Pyrrolidinium Imides: A New Family of Molten Salts and Conductive Plastic Crystal Phases. *J. Phys. Chem. B* **1999**, *103*, 4164−4170.
(18) Rienstra-Kiracofe, J. C.; Tschumper, G. S.; Schaefer, H. F. Atomic and Molecular Electron Affinities: Photoelectron Experiments and Theoretical Computations. *Chem. Rev.* **2002**, *102*, 231−282.
(19) Zhao, Y.; Truhlar, D. G. Density Functionals with Broad Applicability in Chemistry. *Acc. Chem. Res.* **2008**, *41*, 157−167.
(20) Marenich, A. V.; Cramer, C. J.; Truhlar, D. G. Universal Solvation Model Based on Solute Electron Density and on a Continuum Model of the Solvent Defined by the Bulk Dielectric Constant and Atomic Surface Tensions. *J. Phys. Chem. B* **2009**, *113*, 6378−6396.
(21) Frisch, M. J.; Trucks, G. W.; Schlegel, H. B.; Scuseria, G. E.; Robb, M. A.; Cheeseman, J. R.; Scalmani, G.; Barone, V.; Mennucci, B.; Petersson, G. A.; et al. *Gaussian 09*, revision A.02; Gaussian, Inc.: Wallingford, CT, 2009.
(22) Deng, M.-J.; Chen, P.-Y.; Sun, I. W. Electrochemical Study and Electrodeposition of Manganese in the Hydrophobic Butylmethylpyrrolidinium Bis((trifluoromethyl)sulfonyl)imide Room-temperature Ionic Liquid. *Electrochim. Acta* **2007**, *53*, 1931−1938.
(23) Deng, M.-J.; Chen, P.-Y.; Leong, T.-I.; Sun, I.-W.; Chang, J.-K.; Tsai, W.-T. Dicyanamide Anion Based Ionic Liquids for Electrodeposition of Metals. *Electrochem. Commun.* **2008**, *10*, 213−216.
(24) Sanders, J. K. M.; Hunter, B. K. *Modern NMR Spectroscopy*; Oxford University Press: New York, 1988.
(25) Dommert, F.; Schmidt, J.; Qiao, B.; Zhao, Y.; Krekeler, C.; Site, L. D.; Berger, R.; Holm, C. A Comparative Study of Two Classical Force Fields on Static and Dynamics of [EMIM][BF_4] Investigated via Molecular Dynamics Simulations. *J. Chem. Phys.* **2008**, *129*, 224501−224510.
(26) Wakai, C.; Oleinikova, A.; Ott, M.; Weingärtner, H. How Polar Are Ionic Liquids? Determination of the Static Dielectric Constant of an Imidazolium-based Ionic Liquid by Microwave Dielectric Spectroscopy. *J. Phys. Chem. B* **2005**, *109*, 17028−17030.